

# Spatio Temporal Analysis and Simulation Pattern of Land Use and Land Cover Change in Odeda Peri-urban of Ogun State, Nigeria

Anthony Tobore<sup>1\*</sup>, Bolarinwa Senjobi<sup>1</sup>, Ganiyu Oyerinde<sup>2</sup>

<sup>1</sup>Department of Soil Science and Land Management, Federal University of Agriculture Abeokuta, Nigeria.

<sup>2</sup>Department of Soil Science, Faculty of Agriculture, University of Abuja, Nigeria.

Received 5 January 2021; Accepted 4 April 2021

## Abstract

Land use and land cover (LULC) change at the peri-urban is a complex and dynamic process that involves global environmental change. The substantial increase in the human population has led to threats of peri-urban. This study identified the pattern of the LULC change for the years 2014 and 2019 using Landsat satellite images. Soil samples were collected, analyzed, and classified. Principal component analysis (PCA) and Contamination factor (CF) were also determined on the soil nutrients. The Markov Chain (MC) and Cellular Automata (CA) methods were utilized to simulate the LULC maps for the year 2024. Variations among the soil properties decrease across the soil depths and the soils were classified as Mollic Cambisols and Abruptic Eutric. Bioaccumulation index varied substantially with high significant contamination of soil iron. The accuracy of LULC simulation models is more than 85% based on the validation results. The simulation result shows that if the current encroachment continues, the built-up areas will increase by 32% and thus would leading to loss of farmlands and a decrease in food production. Moreover, the rate of economic development in the urban has caused rapid expansion and migration of people into the study area. This study is helpful for planners and decision-makers in ensuring sustainable land-use systems for peri-urban planning.

© 2021 Jordan Journal of Earth and Environmental Sciences. All rights reserved

**Keywords:** land use, land cover, Peri-urban, Markov Chain, Cellular Automata model.

## 1. Introduction

Land use and land cover (LULC) change are some of the major global changes predicted for the future (Su et al., 2012). LULC change at the peri-urban is a complex and dynamic process that involves both natural and human activities (Xiao et al., 2006). LULC is also the primary driving force of sustainable development and global environmental change (Wali et al., 2019). The change in LULC varies from region to region, in rural areas is attributed due to agriculture expansion while in urban areas it is attributed to urban development. The causes and consequences of LULC change are related to human-induced activities which are largely been examined independently (Basommi et al., 2016). Global environmental changes such as emissions of greenhouse gases, global climate change, loss of biodiversity, and loss of soil resources have been closely linked to LULC changes (Li et al., 2016). Additionally, LULC changes are also faced with threats of rapid economic development such as commercialization and urbanization (Hyandye et al., 2017). However, this threat has led to the loss of lands suitable for farming especially in developing countries such as Nigeria (Li et al., 2016).

Studies have shown that urbanization is a major concern of many world regions. It was estimated that the urban population will increase from 3.3 billion in 2007 to 6.4 billion in the year 2050 (United Nations, 2008). Due to this reason, more attention has been given to peri-urban areas as a means to alleviate poverty and ensure food security (Tiani et al., 2015). Globally, about 800 million people engaged

in peri-urban agriculture (FAO, 1999). According to FAO, (2010) peri-urban can be described as “the area of transition between well recognized urban and rural land uses. It has also been conclusively shown that peri-urban contributes to food security (FAO, 2010). Despite their importance, peri-urban are still faced with anthropogenic activities such as discharge of effluents and vicinity dumpsite, etc. (Awoniran et al., 2013).

Monitoring and assessing LULC change at the peri-urban calls for detail and accurate information. Although, assessing LULC changes in developing countries requires urgent attention especially in the spatial environment of today (Tobore et al., 2021). Satellite remote sensing (SRS), in conjunction with Geographic information systems (GIS), have been widely applied and are recognized as an indispensable tool in obtaining accurate and timely spatial data for LULC changes (Mishra et al., 2016; Khan et al., 2016). SRS provides cost-effective valuable information using multispectral and temporal data which is very useful in monitoring and evaluating LULC change (Hua, 2017). For instance: Landsat imagery has been applied extensively for predicting and monitoring LULC change efficiently at different scales and times (Hua, 2017). GIS provides a flexible user environment for collecting, storing, displaying, and analyzing spatial data (Khan et al., 2016). However, the commonly used models for monitoring and predicting LULC changes are Analytical equation-based models (Shamsi, 2010), Statistical models (Hyandye et al., 2017), Evolutionary models (Aitkenhead and Aalders, 2009), Cellular automata

\* Corresponding author e-mail: toboreao@funaab.edu.ng

models (Singh et al., 2015), Markov-chain models (Yang et al., 2012), Expert system models (Stefanov et al., 2001), and Multiagent models (Ralha et al., 2013). At present, the most widely used models in the monitoring and prediction of LULC change are Cellular automata and Markov chain (Sohl and Claggett, 2013; Myint and Wang, 2006). Markov chain models can quantitatively predict the dynamic changes in LULC patterns (Wu et al., 2010). In contrast, cellular automata models can predict the spatial distribution of landscape patterns but cannot predict temporal changes (He et al., 2006). Integration of Cellular automata and Markov chain (CA- Markov) model in LULC studies has advantages such as dynamic simulation capability; high efficiency with spatial and non-spatial data, scarcity and simple calibration; and ability to predicts complex and multiple lands covers patterns (Hyandye et al, 2017; Ansari, 2016). Moreover, many studies have applied CA- Markov model in monitoring and predicting LULC change in the urban (Shahidul Islam and Ahmed, 2011). Thus, few studies have been applied to predict changes in the peri-urban area using the CA - Markov model especially in developing countries such as Nigeria. Hence, this study seeks to integrate the CA-Markov model to evaluate the impacts of LULC change in peri-urban of Odeda Local government area (LGA) of Ogun State, Nigeria. More specifically, the study is targeted to map the spatial and temporal changes in LULC for the years 2014 and 2019. Therefore, the objectives of this study are:

1. To assess, characterize and classify the soil nutrients of the study area.
2. To predicts the LULC change of the study area for 5 years using the CA-Markov model.

## 2. Materials and methods

### 2.1 Description of the study area

The study area is located at Odeda Local Government Area (LGA) of Ogun State, southwestern Nigeria. Odeda falls in the peri-urban area of Abeokuta, close to the city of Ogun State. It falls between latitude  $7^{\circ}49'$  to  $7^{\circ}13'$  and longitude  $3^{\circ}79'$  to  $3^{\circ}14'$  zones 31 North (Figure 1). It has a total surface area of 1,560 km<sup>2</sup> and a population of 109,449 according to the National population census (2006). Agriculture is the main source of occupation and it also

serves as their major livelihood. The crops grown in the area are majorly arable, and permanent crops, such as maize, rice, and oil palm (Dada, 2017).

### 2.2 Climate

The climate of the study area is monsoonal and like all monsoonal climates: it has a contrast between well-defined dry and wet seasons (Adeleye et al., 2020). The wet season lasts from April to October with an annual rainfall of about 2500 mm at the coast and about 1220 mm at the northern limit of the forest belt. The monthly mean minimum temperature is about 22.48°C while the monthly mean maximum temperature is about 31.24°C with an average yearly temperature of about 26.6°C (Adeleye et al., 2020).

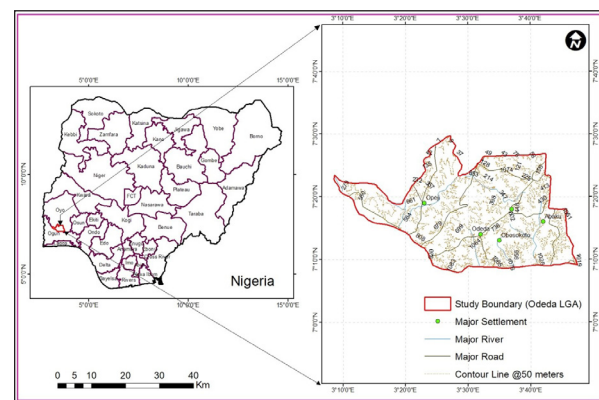


**Figure 1.** The study area (Odeda LGA) showing the contours and some major settlements.

### 2.3 Data Description

Multi-spectral Landsat satellite data for the years 2014 and 2019 were acquired from the United States Geological Survey (USGS) to assess the LULC change. Due to atmospheric error and avoidance of seasonal variation, the Landsat images were downloaded during the period of the dry season. Since the Landsat satellite data are free of radiometric and geometric distortions, there was no additional geo-rectification or image-to-image registration needed for image pre-processing. Information of the images acquired from the USGS online data repository (image type, date, spatial resolution, number of bands, Path and row, and bands composite) are shown in Table 1.

**Table 1.** Details of the Landsat images acquired for the assessment of the Odeda LULC study

Image Type	Acquisition date	Path and row	Bands composite	No of bands	Spatial Resolution
LandSat 7	19/01/2014	P191, R55	432	10	30 Meter
LandSat 8	20/01/2019	P191, R55	652	11	Meter

### 2.4 Multi-temporal land cover mapping

The collected satellite images were enhanced in Idrisi selva Software via (3 by 3) majority filter techniques for better visibility. True Color Composite (TCC) was generated using suitable combinations of bands for the satellite images (d'Entremont and Thomason, 1987; Good and Giordano, 2019). Considering the "Nigeria Land Classification System" and the goal of this study, Anderson and Hardy (1976) classification scheme II and prior knowledge of the study area for over 5 years was used to identify the Area of interest (AOI) features. The images obtained from the Landsat image are classified into 5 LULC classes based

on the Maximum Likelihood Supervised Classification (MLSC) technique (Table 2). The MLCS operation is carried out due to its good performance, visualization, and easy classification algorithm (Liu, 2005; Sun et al., 2013; Biro et al., 2013; Zhang et al., 2015). The accuracies of land cover maps were evaluated using 150 ground truth points from the field and with the support of the year 2019 Google Earth image. These 150 pixels were selected through the random sampling process. The Kappa statistics and confusion matrix was calculated for accuracy assessment (Foody, 2002; Pontius Jr and Millones, 2011; Story and Congalton, 1986).

**Table 2.** The Description of the land categories.

No	Class name	Description
1	Builtup Area	Residential, commercial, industrial services, and transportation network
2	Vegetation	Mixed forest and grass
3	Bareland	Vacant land, open space, sand, bare soils, and landfill sites
4	Farmland	Rainfed cropping planted cropping areas.
5	Waterbodies	River, wetlands, lakes, ponds, and reservoirs.

**2.5 Simulation Pattern Analysis**

To simulate the future LULC pattern of the study area, the Markov Chain (MC) and Cellular automata (CA) model method was applied. MC performs better at modelling LULC in both temporal and spatial dimensions for its higher accuracy (Pontius and Jeffrey, 2007). CA underlies the dynamics of LULC change for any location (cells) based on the concept of proximity (Balogun and Ishola, 2017). The CA-Markov model was implemented in the Landsat images of the years 2014 and 2019 in the Idrisi Selva environment (Tobore et al., 2021). The LULC change prediction was based on the dependent and independent variables. The dependent variable used includes the Digital elevation model (DEM), aspect, distance from a major road, and distance from the river (Figure 2a and 2b). The DEM and aspect were derived from the Shuttle radar topographic mapper (SRTM) of 30-meter resolution downloaded from the USGS website. The DEM ranges from the lowest value of 33 meters to the highest value of 266 meters from mean sea level (MSL) in the study area. The aspect maps indicate a more or less flat surface presence in the study area. Distance from major roads and rivers were derived from vector layers from an open street map. The analysis of the dependent variable was carried out using the ArcGIS 10.5 environment using Euclidean distance operation. The independent variables are the LULC of the year 2014 and 2019 classification maps. The independent and dependent variables were used as input parameters to generate the transition probability matrix. The transition matrix analysis generates an empirical likelihood image that estimated the probability of change between LULC in the study area. The random sampling method was applied using the maximum iteration and neighbourhood of 3 by 3 cells i.e. 9 cells. The Cellular automata and Markov Chain were predicted according to Ma et al. (2016):

$$S_{t+1} = P_{ij} \times S_t \dots\dots\dots \text{Eq. 1}$$

Where: : represent the land-use status

T, and t+1 represent the time point

$P_{ij}$ : represent the state transition probability matrix

$$P_{ij} \begin{bmatrix} P_{11}, & \dots & P_{11}, P_{11} \\ \dots, & \dots & \dots \\ P_{11} & P_{11} & P_{11} \end{bmatrix} \dots\dots\dots \text{Eq. 2}$$

**2.6 Accuracy assessment**

To ensure the validity of the model for predicting LULC change for the projected year, a validation process was performed using the existing database. The CA-Markov model was validated to simulate the LULC of the year 2019, which is compared to the estimated LULC map of the same year. The validation process was performed in the Idrisi

selva environment producing several Kappa (K) parameters: kappa for grid cell level location (Klocation), kappa for no information (Kno), kappa for stratum-level location (KlocationStrata), and kappa standard (Kstandard) following the standard procedure of Pontius Jr and Millones (2011).

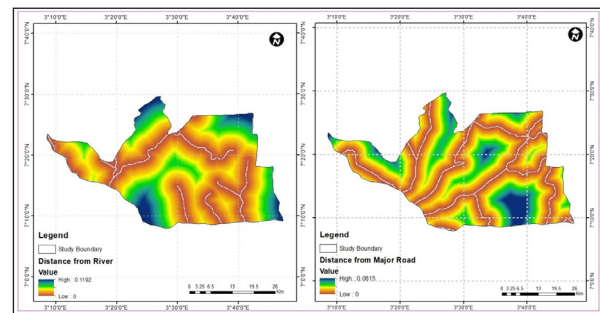


**Figure 2a.** The study area (Odeda LGA) showing the distance from Major Road and River.

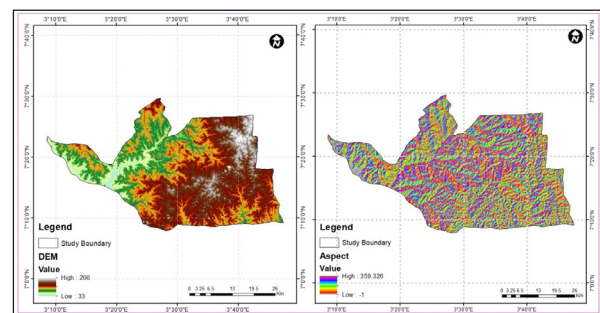


**Figure 2b.** The study area (Odeda LGA) showing the digital elevation model and Aspect.

**2.7 Vegetation Cover analysis**

Vegetation indices derived from satellite remote sensing data are one of the primary sources of information for monitoring the Earth’s vegetation cover (Gilabert et al., 2002). Vegetation indices are usually developed to extract vegetation information from two or more spectral bands. In this study, LULC changes were assessed with Soil adjusted vegetation index (SAVI) for the years 2014 and 2019. SAVI has a better efficiency to calculate vegetation index by reducing the influence of soil background (Gilabert et al., 2002). Afterwards, SAVI was used to identify significant changes in the vegetation cover of the study area. The equation is given by (Huete, 1988):

$$SAVI = \frac{(NIR - RED)}{NIR + RED + L} (1 + L) \dots\dots\dots \text{Eq. 3}$$

where: NIR represents the spectral reflectance measurements in the near-infrared regions of band 5; Red represents the Spectral reflectance measurements in the visible red of the band 4 and L is the constant or correction factor, ranges from 0 to 1.

**2.8 Soil mapping**

The study area was sampled using reconnaissance and stratified grid sampling. The slopes from which transects were cut for soil mapping include pedon 1 (Odeda), pedon 2 (Olodo), and pedon 3 (Isolu). Soil sampling was collected at the soil depth of 0 -15cm and 15 – 30cm for soil analysis. A total number of 74 soil samples were collected for this study. Soil sampling coordinate point was recorded using a Global positioning system (GPS). At each pedon, representative soil profile pits measuring 2 m by 1.5 m by 2 m (meters) were dug at the predominant slope i.e. Crest, middle and lower slope. A total of 9 soil profile pits were dug and described based on soil morphology, chemical, and physical which was suggested by FAO, (2009) procedure. Soil samples were collected from the different pedogenic horizons and then processed in the laboratory after air-drying at room temperature.

**2.9 Soil classification**

Based on morphological characteristics and laboratory data of the soil mapping, the soils of the study area were classified using the USDA Soil Taxonomy (Soil Survey Staff, 2010) and the World Reference Base (WRB) system of FAO/IUSS Working Group (2006).

**2.10 Soil pollution load assessment model**

Pollution by soil heavy metals has been widely studied using several indices (Odukoya et al., 2016). In this study, the Contamination factor (CF) index was used to assess the soil heavy metal concentration. CF is used to assess contamination level relative to the average concentration of the respective heavy metals in the environment i.e. soil to the measured background values from the previous study with similar geological origin or uncontaminated soil (Sutherland, 2000; Tijani et al., 2004; Uriah and Shehu, 2014). The CF is often expressed based on the formula previously described by Hakanson (1980) and has been applied by Odukoya et al. (2016).

$$CF = \frac{C \text{ metal}}{C \text{ Bkg}} \dots\dots\dots \text{Eq. 4}$$

Where C: metal represents the concentration (mg/kg<sup>-1</sup>) of a given heavy metal in soil

C Bkg: represent the background or preindustrial concentrations (mg/kg<sup>-1</sup>).

**2.11 Geospatial mapping of soil heavy metals**

Among the metal concentration, iron (Fe), zinc (Zn), and manganese (Mn) were selected to assess the level of heavy metals using 0 -15 cm soil depth. According to Obiora et al. (2016), Fe, Zn, and Mn are the most common contaminated heavy metals found in Nigeria’s soils and environment. The collected coordinates of the soil heavy metals concentration were processed in an excel spreadsheet and saved as text delimited. Each of these metal concentrations was plotted and display in the ArcMap. Thereafter, the Inverse difference weight (IDW) technique was used for the interpolation of soil data according to Li and Heap (2008). Raster calculator tool in ArcGIS 10.5 environment was used to assess the formula described by Odukoya et al. (2016) for soil concentration mapping for the study area. Due to no data information of

preindustrial or preanthropogenic activities in southwestern Nigeria, geochemical background concentration values of 9 mg/kg<sup>-1</sup> were used to assess the quality of the soil in the study area according to Pejman et al. (2009) as described in table (3).

**Table 3.** Geochemical and pollution indices

Classes	Pollution Intensity	Soil Quality
0-1	0	Unpolluted
1-2	1	Unpolluted to moderately polluted
2-3	2	Moderately polluted
3-4	3	Moderately to highly polluted
4-5	4	Highly polluted
5-6	5	Highly to very highly polluted
6-7	>5	Very highly polluted

Source: Pejman et al. (2009)

**2.12 Soil samples analysis**

The soil samples were air-dried and passed through a 2mm diameter sieve before analysis for the soil’s physical and chemical properties. Afterwards, soil pH was determined in potassium chloride and water suspensions with a glass electrode pH meter (McLean et al., 1982). Soil organic carbon (OC) was determined by the chromic acid oxidation method (Walkley and Black, 1939). The total nitrogen (TN) of the soil was determined by the macro Kjeldahl method. The soil available phosphorus (P) was determined according to the Bray-1 method. Exchangeable bases Calcium, Magnesium, Potassium, and Sodium (Ca<sup>2+</sup>, Mg<sup>2+</sup>, K<sup>+</sup> and Na<sup>+</sup>) in the soil were extracted with 1 N ammonium acetate solution. The Ca<sup>2+</sup> and Mg<sup>2+</sup> were determined with atomic absorption spectrophotometer (AAS) while (K<sup>+</sup>) and (Na<sup>+</sup>) were read on a flame photometer. Exchangeable acidity (H<sup>+</sup>) in the soil was extracted with 1N Kcl and measured using the titration method (Anderson and Ingram, 1993). Effective cation exchange capacity (ECEC) was estimated by the summation of the exchangeable acidity and exchangeable bases. Base saturation (BS) was calculated as the percentage ratio of the exchangeable bases to the ECEC following the procedure of Udo et al. (2009). The particle size distribution of the soil was determined by the hydrometer method (Bouyoucos, 1962). For heavy metal analyses, sub-samples (0.5 g) of each of the soil were digested. Digestion was done with 10 ml of a mixture of nitric (HNO<sub>3</sub>) and perchloric (HClO<sub>4</sub>) acid in ratio 2:1 (v/v) for 90 min, initially at 150° C. After which 2ml of concentrated HCL was added to the mixture. The temperature of the digest was then increased to 230° C for another 30 minutes on the digester. On completion of digestion, digests were allowed to cool down at room temperature. Thereafter, the content of each digestion tube was transferred into a 50 ml volumetric flask and made to volume with distilled water.

**2.13 Statistical analysis**

The relationship across the soil nutrients was subjected to Principal component analysis (PCA), correlation, and regression analysis using R- statistics v4.0.3. The correlation coefficients were estimated for all possible variable combinations to generate a correlation matrix.

### 3. Results and Discussion

#### 3.1 Land use/cover mapping

Periodical assessment characteristics and colour composite were used to classify the LULC change of the studied area. Results of the MLSC algorithm for evaluating LULC changes between the year 2014 and 2019 patterns are presented in Figure (3) and (4). Overall classification accuracy of MLSC was 94.10% and 95.87% in the years 2014 and 2019 respectively (Table 4). For validation, the predicted LULC map of 2019 was compared with the observed LULC map of 2019 using kappa index statistics. Based on the evaluation of predicted LULC with observed LULC scenarios, a kappa statistic for quantity and location was derived. The statistics showed that Kno, Klocation, KlocationStrata, and Kstandard values were 0.8603, 0.8869, 0.8743, and 0.8645 (overall kappa), respectively. After the prediction, it was found out that all kappa index values were  $> 0.86$  showing high agreement between predicted and observed LULC maps. The statistical analysis of the multi-temporal LULC maps revealed that significant changes have occurred. From the change analysis of LULC between 2014 and 2019, it was observed that there was an increase in farmland, built-up, bare land, and water bodies with a value of 30.80%, 20.18%, 17.63%, and 1.92% respectively while vegetation was decreased from 60.51% to 29.43% (Table 5).

To predict future LULC change, the land use map of 2014 and 2019, and then the output was used to predict future LULC for the year 2024 using the CA-Markov model (Figure 5). The significant changes that are predicted to occur between 2019 and 2024 would be due to the conversion of bare land, water bodies, and vegetation. Therefore, change analysis of LULC between 2019 and 2024 indicated that built-up and farmland will increase in the order of 163.87 ha (Hectare) and 124.36 ha, while bare land, vegetation, and water bodies were decreased by -140.13ha, 132.67ha, and -15.43ha, respectively (Table 6). The results revealed that a sudden increase in farmland and built-up area can be attributed to a substantial increase in human activities. Besides, the increase observed in farmland could also be traced to the over-exploitation of land resources which serves as a means of livelihood and source of occupation for the majority of people living in the peri-urban area. Also, an increase in the built-up area by the next 5 years, may lead to more people migrating from urban to peri-urban due to unplanned population growth in the city. However, the main reason for these changes could be attributed to some factors such as agricultural land use expansion, biodiversity loss, pollution of water and soils in the studied area. Weng and Yang (2004) pinpointed that both geopolitical and economic factors contribute to the increases in human activities and thus leading to built-up expansion. Adepaju et al. (2006) also stated that LULC change has been recognized as an important driver of global environmental changes. The present study also corroborates with Nachtergaele et al. (2011) who found out that peri-urban areas are rapidly experiencing biodiversity decrease and high human activities thereby leading to the sudden decrease in vegetation cover and built-up expansion. However, further studies supporting this study results can be found in Bankole and Bakare (2011).

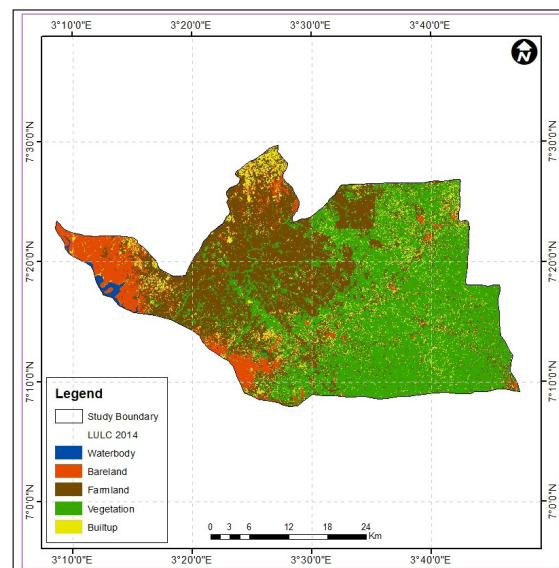


Figure 3. The study area (Odeda LGA) showing the year 2014 LULC changes.

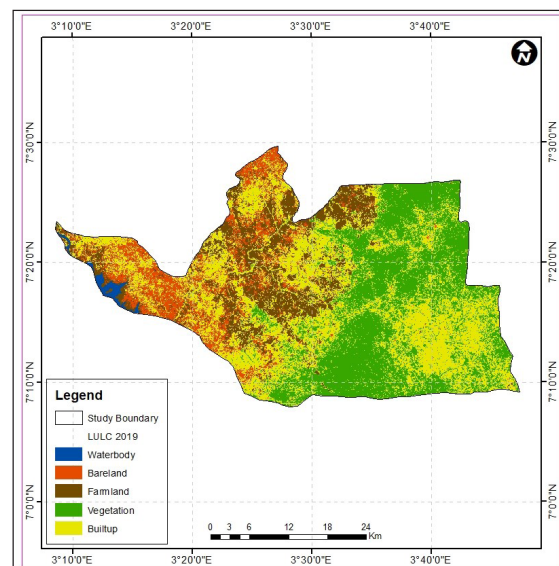


Figure 4. The study area (Odeda LGA) showing the year 2019 LULC changes.

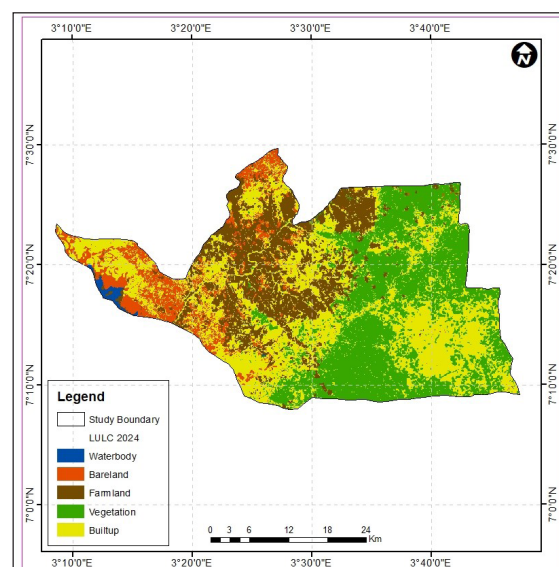


Figure 4. The study area (Odeda LGA) showing the year 2019 LULC changes.

**Table 4.** Accuracy assessment of the LULC classified maps (Odeda LGA) for the years 2014 and 2019.

LULC	User Accuracy (%)						Overall Classified Accuracy	Producer Accuracy (%)					Overall Statistic Kappa
	WB	BL	VG	FD	BA	WB		BA	VG	FD	BA		
2014	98.4	98.9	98.5	94.3	97.2	94.10%	98.5	96.4	95.8	88.8	95.3	0.9488	
2019	98.2	97.5	98.7	94.9	96.5	95.87%	99.8	95.9	88.2	96.8	97.5	0.9365	

LULC: WB: Waterbodies; BL; Bareland; FD: Farmland; VG; Vegetation; BA

**Table 5.** Change analysis of LULC (Odeda LGA) between the years 2014 and 2019.

LULC	Area in 2014		Area in 2019		Change in 2014 -2019 (ha)
	(ha)	(%)	(ha)	(%)	
Waterbodies	18.33	1.34	26.32	1.92	7.99
Bareland	135.21	9.90	240.82	17.63	105.61
Farmland	256.93	18.81	420.63	30.80	163.70
Vegetation	826.14	60.51	401.89	29.43	- 424.25
Builtup	128.66	9.42	275.61	20.18	146.95
Total	1365.27	100	1365.27	100	

**Table 6.** Change analysis of LULC(Odeda LGA) between the years 2019 and 2024.

LULC	Area in 2019		Area in 2024		Change in 2019 -2024 (ha)
	(ha)	(%)	(ha)	(%)	
Waterbodies	26.32	1.92	10.89	0.79	-15.43
Bareland	240.82	17.63	100.69	7.37	-140.13
Farmland	420.63	30.80	544.99	39.91	124.36
Vegetation	401.89	29.43	269.22	19.71	-132.67
Builtup	275.61	20.18	439.48	32.18	163.87
Total	1365.27	100	1365.27	100	

**3.2 Satellite-based vegetation Assessment**

Vegetation indices have been used to monitor temporal changes associated with vegetation and spectral reflectance (Gilabert et al., 2002). One of these commonly used vegetation indices is the SAVI. SAVI appears to be more reliable and less noisy than the NDVI (Normalized difference vegetation index) (Waswa et al., 2012). In this study, the SAVI vegetation index was used and the vegetation cover ranged from -0 to 0.2715 for the year 2014 and 0 to 0.0317 for the year 2019 (Figure 6). The results revealed that during the year 2019, low vegetation-covered was experienced when compared to that of the year 2014. The effects of the low vegetation observed in the year 2019 might be traced to the rate of human activities experienced in the study area such as farmland and built up expansion. Additionally, indiscriminate grazing of cattle might also be responsible for the low vegetation observed in the year 2019 especially during the dry season when the chlorophyll content is low.

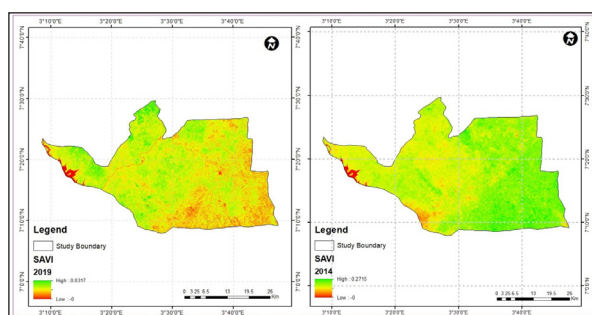


**Figure 6.** The study area (Odeda LGA) showing the year 2014 and 2019 soil adjusted the Vegetation index.

**3.3 Soil fertility variation at 0 -15cm depth**

As shown in Figure 7, cluster variations were observed among the chemical soil properties. The soil zinc (Zn) was observed along the same dimension (dimension 2) with exchangeable acidity and iron (Fe). This simply means that as Zn decreases exchangeable acidity and soil iron also decrease. The exchangeable bases; magnesium (Mg), sodium (Na), potassium (K), and effective cation exchanged capacity (ECEC) were also observed along the same dimension (dimension 3). This confirms the fact that an increase in exchangeable bases will lead to higher ECEC in the studied soil. The soil pH, available phosphorus (P), soil total nitrogen (TN), and soil organic carbon (OC) were found in the same dimension. The calcium, soil Fe, Mg, and base saturation also behaved the same way.

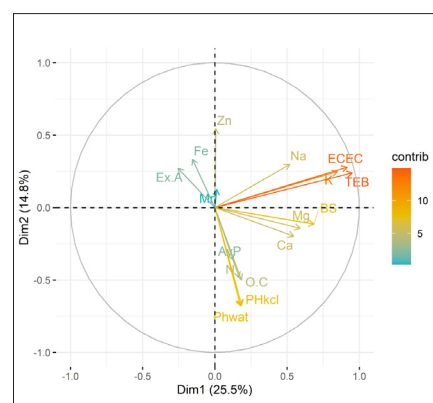


**Figure 7.** Variable factor map of Principal component analysis for soil sampled at 0 - 15cm depth.

3.4 Correlation among soil properties at 015-cm.

From Table 7, high R squared (R<sup>2</sup>) values were observed among soil OC versus TN, K versus Total exchangeable bases (TEB), ECEC, and TEB versus ECEC (Figure 8 - 10). The linear regression plots and modelling equation shows how the soil properties could be predicted in the study area (Table, 7).

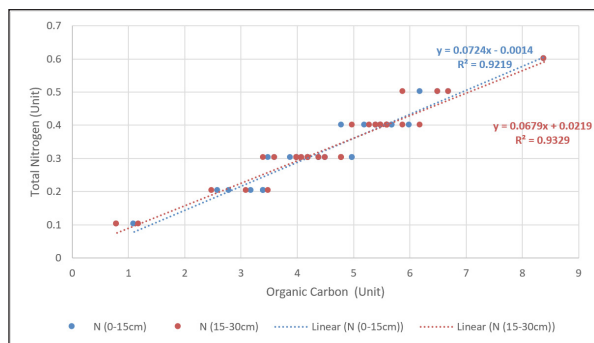


Figure 8. The study area (Odeda LGA) showing the linear regression between Nitrogen and Organic Carbon.

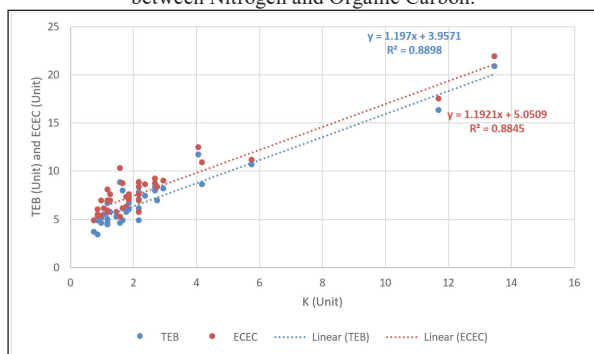


Figure 9. The study area (Odeda LGA) showing the linear regression among K versus TEB/ECEC.

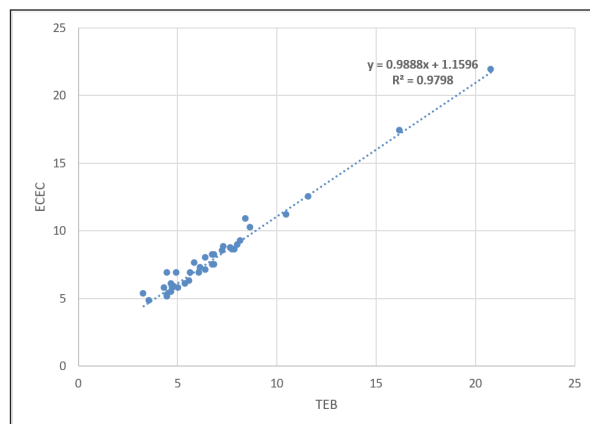


Figure 10. The study area (Odeda LGA) showing the linear regression between TEB and ECEC.

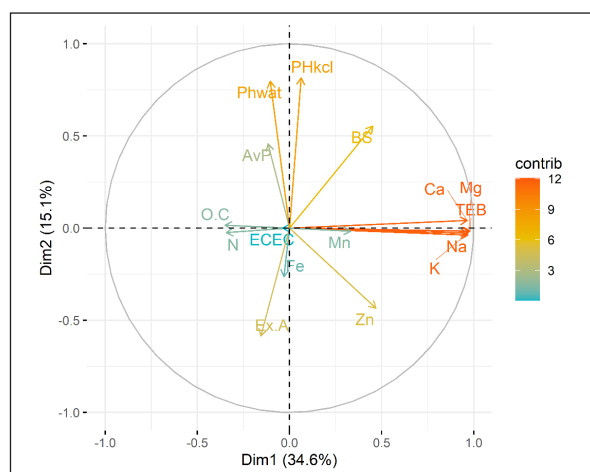


Figure 11. The study area (Odeda LGA) showing the variable factor map of principal component analysis for soil samples at 15-30 cm.

Table 7. The study area (Odeda LGA) showing the R2 correlation among soil properties at 0-15cm soil depth.

	O.C	AvP	N	Ex.A	Na	K	Ca	Mg	TEB	ECEC	BS	pHkcl	pHwater	Fe	Zn
AvP	0.029														
N	0.922	0.028													
Ex.A	0.001	0.046	0.000												
Na	0.004	0.044	0.002	0.001											
K	0.011	0.014	0.020	0.001	0.108										
Ca	0.019	0.002	0.001	0.099	0.005	0.059									
Mg	0.002	0.003	0.000	0.001	0.048	0.108	0.270								
TEB	0.009	0.002	0.010	0.006	0.298	0.890	0.159	0.205							
ECEC	0.008	0.000	0.010	0.004	0.304	0.884	0.126	0.210	0.980						
BS	0.001	0.029	0.000	0.666	0.108	0.177	0.227	0.065	0.290	0.179					
pHkcl	0.001	0.043	0.001	0.020	0.004	0.000	0.006	0.039	0.001	0.000	0.026				
pHwater	0.003	0.028	0.009	0.027	0.004	0.000	0.022	0.033	0.000	0.000	0.034	0.578			
Fe	0.013	0.010	0.006	0.077	0.028	0.000	0.008	0.083	0.008	0.017	0.026	0.138	0.058		
Zn	0.030	0.009	0.032	0.000	0.002	0.011	0.000	0.018	0.008	0.008	0.001	0.101	0.022	0.045	
Mn	0.035	0.196	0.022	0.000	0.003	0.002	0.000	0.001	0.000	0.000	0.001	0.000	0.022	0.022	0.158

3.5 Correlation among soil properties at 15 -30cm depth

In Figure 11, Soil O.C and N followed a similar direction which indicates correlation among the soil properties and thus affected by the same factors. Both soil pH (water and potassium chloride) along with available P is found around

dimension 2. All the Exchangeable bases (Ca, Mg, Na, K, and Mn) and TEB have good relationships as displayed in dimensions 2 and 3. In line with the PCA, soil O.C and N have a high correlation. The exchangeable bases also showed great relationships as highlighted in yellow (Table 8).

**Table 8.** The study area (Odeda LGA) showing the R2 correlation among soil properties at 15-30cm.

	O.C	AvP	N	Ex.A	Na	K	Ca	Mg	TEB	ECEC	BS	pHkcl	pHwater	Fe	Zn
AvP	0.044														
N	0.933	0.029													
Ex.A	0.015	0.108	0.039												
Na	0.040	0.026	0.034	0.001											
K	0.053	0.016	0.043	0.003	0.925										
Ca	0.038	0.007	0.032	0.011	0.917	0.916									
Mg	0.048	0.012	0.040	0.003	0.965	0.952	0.965								
TEB	0.047	0.016	0.039	0.004	0.969	0.985	0.959	0.985							
ECEC	0.011	0.024	0.013	0.012	0.004	0.002	0.007	0.017	0.000						
BS	0.013	0.032	0.034	0.648	0.129	0.147	0.157	0.108	0.145	0.093					
pHkcl	0.002	0.041	0.001	0.033	0.006	0.002	0.009	0.005	0.004	0.001	0.054				
pHwater	0.004	0.037	0.002	0.021	0.012	0.008	0.002	0.007	0.008	0.001	0.030	0.602			
Fe	0.002	0.009	0.006	0.068	0.008	0.003	0.011	0.008	0.006	0.004	0.019	0.135	0.117		
Zn	0.010	0.020	0.007	0.008	0.167	0.156	0.135	0.142	0.157	0.013	0.007	0.075	0.094	0.032	
Mn	0.048	0.161	0.091	0.002	0.060	0.043	0.057	0.060	0.052	0.017	0.007	0.000	0.008	0.012	0.150

### 3.6 Soil Mapping of the (Odeda LGA) study area

The diagnostic criteria of the pedons were classified according to the USDA Soil Taxonomy (Soil Survey Staff, 2010) and World Reference Base for Soil Resources (FAO/ISRIC/IUSS, 2006). The differentiating properties used for the soil classification include physical, chemical, and morphological soil properties. The particle size distribution classification indicated that the soil texture ranged from sandy to sandy loam. The high preponderance of sand indicated a dominance of low activity clay such as kaolinite. There was a consistent clay increase across the pedons leading to the formation of the argillic horizon. The soils were strongly acidic to neutral with a soil pH ranging from 5.1 to 7.3. Available phosphorus (< 8 to 20 mg/kg), and total nitrogen ranged from low to medium (<0.1 to 0.2%). Organic carbon had higher levels (1.0 to >20%) in the analyzed soils. The high content of soil OC observed could be traced to the presence of deposition or dumping of waste material into the vicinity of the studied area. ECEC of the soils is more than 1.5 cmol/kg<sup>-1</sup> in the studied soils and this may be responsible for the intense leaching of the exchangeable cations due to the parent material.

### 3.7 Soil Classification of the (Odeda LGA) study area

All the pedons were well-drained and dry for as long as 90 cumulative days with a mean annual soil temperature of 22°C, thus considered as Udic moisture regime and classified as Isohyperthermic. This is also in consonance with the work done by Amusan and Ashaye (1991) which states that soil temperature regime in Southwestern - Nigeria can be classified as isohyperthermic. The pedons had base saturation of > 50% with a colour value from < 4 and chroma 3 or less, and soil OC content of more than 0.6% (Soil Survey Staff, 2010). This implies that the studied soils can be considered as mollic Epipedon. At the Order level, pedons 1 and 2 were classified as Inceptisol due to little or no soil profile development across the horizons (Soil Survey Staff, 2010), while at pedon major processes such as erosion, and highly leached soils due to slope position (>2 mm in

diameter) were observed and therefore classified as Ultisols. At the suborder level, there was high sandy distribution and irregular clay movement down the horizon at the soil profile. Therefore, at the suborder, the soils can be classified as Typic Kandiodult with ECEC of more than 1.5 cmol/kg<sup>-1</sup>. According to the World Reference Base for Soil Resources, pedons 1 and 2 were classified as Mollic Cambisols (Endo – Skeleton, Eutric) due to the beginning or incipient subsurface horizon differentiation and alteration while pedon 3 were classified as Haplic Gleysols (Abruptic, Eutric) due to saturated groundwater and gleyic colour pattern (FAO/ISRIC/IUSS, 2006).

### 3.8 Geoconcentration of heavy metals in studied (Odeda LGA) soils

The assessment of pollution levels of heavy metals soil contamination is significant to human health and environmental management. In this study, the soil heavy metals were interpolated and classified according to Pejman et al. (2009) soil quality. The order of contribution of the heavy metals to soil contamination increased in the following order: Fe > Mn > Zn. The overall pollution load index indicated that the soils ranged from unpolluted to highly polluted (Figure 12). The soil heavy metal reveals that vicinity waste and effluent discharge into rivers and streams could be responsible for the rate of contamination in the studied soils. According to Mazurek et al. (2017), heavy metals pollution in the soil varies according to its chemical and physical characteristics including texture, and buffering ability. Mazurek et al. (2017) and Pająk et al. (2015) also reported that the distribution and arrangement of soil heavy metals depend on landscape and/or topography. Hence, this could account for variation found among the soil heavy metals. The results are also in consonance with the studies of Ajmone-Marsan and Biasioli (2010) as well as that of Obiora et al. (2016) who reported that soil Fe, Mn, and Zn are among the most common contaminated heavy metals found in Nigeria soils and environment.

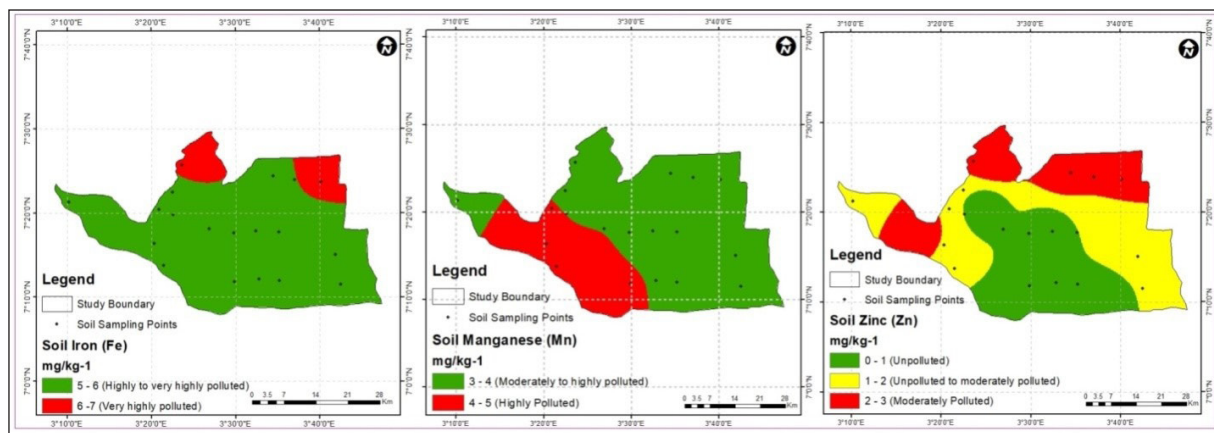


**Figure 12.** The study area (Odeda LGA) showing the Geoconcentration of soil iron, manganese, and zinc.

#### 4. Conclusions

The study objective was to evaluate the significance of LULC change from the year 2014 to 2024 using GIS, RS data, and the CA-Markov model in Odeda LGA, Ogun State, Nigeria. Prediction of future LULC changes at the study area can help to manage the sudden encroachment. The finding reveals that built-up area and farmland was increased by 32.18% and 39.91% from the year 2014 to 2019, which leads to a decrease in vegetation by (19.71%), bareland (7.37%), and water bodies (0.79%). The increase in built-up area and farmland could be attributed to the increase in human activities such as built-up expansion through the sudden encroachment of people migrating from urban to the study area. The soil nutrients variation shows a good relationship and decreases across the soil depths. Concentrations of soil Zn, Fe, and Mn in the study soils varied substantially with high significant contamination of soil Fe. The rate of human activities such as vicinity dumpsite, and discharge of industrial waste into the streams and river can lead to the transferring of toxic metals to the food chain; thereby leading to a potential risk to human health and a decrease in food production in the studied area. The present study demonstrated the efficiency of GIS and RS data in the study of LULC change using the Cellular Automata and Markov chain model.

#### Acknowledgements

The authors are sincerely grateful to farmers in the study area for their understanding and for allowing us to carry out this study on their farms. We are equally thankful to the USGS for assisting this research with data sets.

#### Funding

This research did not receive any specific grant from funding agencies in the public, commercial, or not-for-profit sectors.

#### References

Adeleye, N., Osabuohien, E., Adeogun, S., Fashola, S., Tasiye, O., Adeyemi, G. (2020). Access to Land and Food Security: Analysis of 'Priority Crops' Production in Ogun State, Nigeria. In, Osabuohien, E (Ed.), *The Palgrave Handbook of Agricultural and Rural Development in Africa* (pp. 291-311). Cham-Switzerland: Palgrave Macmillan. DOI: [https://doi.org/10.1007/978-3-030-41513-6\\_14](https://doi.org/10.1007/978-3-030-41513-6_14).

Adepoju, M.O., Millington, A.C., Tansey, K.T., (2006). Land Use/Land Cover Change Detection in Metroplitian Lagos (Nigeria): 1984-2000. AASPRS 2006 Annual Conference, Reno Nevada, May 1-5, 2006, Maryland: American Society for Photogrammetry and Remote Sensing.

Ajmone-Marsan, F., and Biasioli, M.(2010).Trace elements in soils of urban areas. *Water, Air, and Soil Pollution* 213: 121–143. DOI: 10.1007/s11270-010-0372-6.

Amusan, A.A., and Ashaye, T.I. (1991). Granitic-gneiss derived soils in humid forest tropical southwestern Nigeria I: Genesis and classification. *Ife Journal of Agriculture* 13 (1-2): 1 – 20.

Anderson, J.M., and Ingram, J.S.L. (1993). *Tropical soil biology and fertility: handbook of Method of Analysis*. UK:International Wallingford, (pp. 38–39).

Anderson, J.R., and Hardy, E.E. (1976). *A Land Use and Land Cover Classification System for Use with Remote Sensor Data*. Geological Survey Professional.

Ansari, A. (2016). The final report of the research project "Identification of harvesting centres' and effective factors of dust storms in Michigan Desert Wetland" Arak University.

Aitkenhead, M.J., and Aalders, I.H. (2009). Predicting land cover using GIS, Bayesian and evolutionary algorithm methods. *Journal of Environmental Management* 90(1): 236–50. <https://doi.org/10.1016/j.jenvman.2007.09.010> PMID: 18079039.

Awoniran, D.,R., Adewole, M.B., Adegboyega, S.A, Anifowose, A. Y. B. (2013). Assessment of environmental responses to land-use / land-cover dynamics in the lower Ogun River Basin, South-western Nigeria. *International Journal of Sustainable Land use and Urban Planning* 1(2):16-31.

Balogun, I., and Ishola, K. (2017). Projection of future changes in land-use/ land-cover using cellular automata/Markov model over Akure city, Nigeria. *Journal of Remote Sensing Technology* 5 (1): 22–31.

Bankole, M.O., and Bakare, H.O. (2011). Dynamics of urban land-use changes with remote sensing: Case of Ibadan, Nigeria. *Journal of Geography and Regional Planning* 4(11): 632-643.

Basommi, L.P., Guan, Q.F., Cheng, D.D., Singh, S.K. (2016). Dynamics of land-use change in a mining area: a case study of Nadowli District, Ghana. *Journal of Mountain Science* 13(4): 633–42. <https://doi.org/10.1007/s11629-0153706-4>.

Biro, K., Pradhan, B., Buchroithner, M., Makeschin, F.(2013). Land use/Land cover change analysis and its impact on soil properties in the northern part of Gadarif region, Sudan. *Land Degradation and Development* 24(1): 90–102. <https://doi.org/10.1002/ldr.1116>.

Bouyoucos, G.H. (1962). Hydrometer method for making particle size analysis of soils. *Agronomy Journal* 54: 464-465. DOI: 10.2134/agronj1962.00021962005400050028x.

- Dada, S. (2017). Public-Private Dialogue Report on Land Administration, Registration and Acquisition in Ogun State. Nigeria: Deutsche Gesellschaft für Internationale Zusammenarbeit (GIZ).
- D'Entremont, R.P., and Thomason, L.W. (1987). Interpreting meteorological satellite images using a colour-composite technique. *Bulletin of the American Meteorological Society* 68(7): 762-768.
- FAO-ILASA-China-Dokuchaev (1999). CD-ROM on Soil and Terrain Database for North and Central Eurassia (Version 1.0), FAO, ROME.
- FAO/IUSS Working Group (2010). A framework for land evaluation. Rome: Soils Bulletin 31, pp 25-42.
- FAO, Rome (2006). The State of Food Insecurity in the World. Food and Agriculture Organization of the United Nations, Rome.
- FAO, Rome (2009). The State of Food Insecurity in the World. Food and Agriculture Organization of the United Nations, Rome.
- Foody, G.M. (2002). Status of land cover classification accuracy assessment. *Remote Sensing of Environment* 80 (1): 185–201.
- Gilbert, M. A., González-Piqueras J., García-Haro F. J., Meliá J., (2002). "A generalized soil-adjusted vegetation index." *Remote Sensing of Environment* 82(2):303-310. DOI:10.1016/S0034-4257(02)00048-2.
- Good, T., and Giordano, P.A., (2019). Methods for Constructing a Color Composite Image: Google Patents.
- He, C., Okada, N., Zhang Q., Shi, P., Zhang, J. (2006). Modeling urban expansion scenarios by coupling cellular automata model and system dynamic model in Beijing, China. *Applied Geography* 26(3): 323–45. <https://doi.org/10.1016/j.apgeog.2006.09.006>.
- Hua, A.K. (2017). Analytical and Detection Sources of Pollution Based Environmetric Techniques in Malacca River, Malaysia. *Applied Ecology and Environmental Research* 15 (1): 485-499.
- Hakanson, L. (1980). An ecological risk index for aquatic pollution control of sediment ecological approach. *Water Research* 14: 975–1000.
- Huete, A.R. (1988). A soil-adjusted vegetation index (SAVI). *Remote Sensing of Environment* 25: 295-309.
- Hyandye, C, Mandara, G., Safari, J. (2017). GIS and Logit Regression Model Applications in Land Use/Land Cover Change and Distribution in Usangu Catchment. *American Journal of Remote Sensing* 3(1): 6–16. doi: 10.11648/j.ajrs.20150301.12.
- Pejman, A.H., Bidhendi, G.R.N., Karbassi, A.R., Mehrdadi, N., Bidhendi, M.E. (2009). Evaluation of spatial and seasonal variations in surface water quality using multivariate statistical techniques. *International Journal of Environmental Science and Technology* 6: 467–476 (2009). DOI: 10.1007/BF03326086.
- Khan, S., Cao, Q., Zheng, Y.M., Huang, Y.Z., Zhu, Y.G. (2016). Health risks of heavy metals in contaminated soils and food crops irrigated with wastewater in Beijing, China. *Environmental Pollution* 152(3): 686–692. <https://doi.org/10.1016/j.envpol.2007.06.056>.
- Li, X., Min, X.U., Cao, C., Singh, P.R., Chen, W., Ju, H. (2016). Land use and land cover changes and their influence on the Ecosystem in Chengdu City during the period of 1982 – 2018. *Sustainability* 10: 3580.
- Li, J., and Heap, A.D. (2008). A Review of Spatial Interpolation Methods for Environmental Scientists. *Geoscience Australia, Record* 2008/23, 137 pp.
- Liu, H. (2005). Accuracy analysis of remote sensing change detection by rule-based rationality evaluation with post-classification comparison. *International Journal of Remote Sensing* 25(5): 1037–1050. <http://dx.doi.org/10.1080/0143116031000150004>.
- Ma, X., Zuo, H., Tian, M., Zhang, L., Meng, J., Zhou, X., Min, N., Chang, X., Liu, Y. (2016). Assessment of heavy metals contamination in sediments from three adjacent regions of the Yellow River using metal chemical fractions and multivariate analysis techniques. *Chemosphere* 144:264-72. DOI: 10.1016/j.chemosphere.2015.08.026.
- McLean, E. O., Dumford, S. W. F., Coronel, S.W. (1982). A comparison of several methods of determining lime requirements of the soil. *Soil Science Society of America Journal* 30(1): 26-30.
- Mazurek, R., Kowalska, J., Gasiorek, M., Zadrozny, P., Jozefowska, A., Zaleski, T. (2017). Assessment of heavy metals contamination in surface layers of Roztocze National Park forest soils (SE Poland) by indices of pollution. *Chemosphere* 168: 839–850.
- Mishra, V.N., Rai, P.K., Kumar, P., Prasad, R. (2016). Evaluation of land use/land cover classification accuracy using multi-resolution remote sensing images. *Geographic Forum* XV(1):45–53. <https://doi.org/10.5775/fg.2016.137.i>.
- Myint S.W., and Wang, L. (2006). Multicriteria decision approach for land use land cover change using Markov chain analysis and a cellular automata approach. *Canadian Journal of Remote Sensing* 32(6): 390–404. <https://doi.org/10.5589/m06-032>.
- Nachtergaele, F.O., Velthuisen, H., Van, Verelst, L., Batjes, N.H., Dijkshoorn, J.A., Engelen, V.W.P. van, Fischer, G., Montanarella, L., Petri, M., Prieler, S., Teixeira, E., Wilberg, D., Shi, X. (2011). World Soil Database. Version 1.0. <http://www.fao.org/nr/water/docs/Harm-World-Soil-DBv7cv.pdf> (accessed November 2015).
- National Population Commission, Nigeria (2006). Census Report.
- Obiora, S.C., Chukwu, A., Davies, T.C. (2016). Heavy metals and health risk assessment of arable soils and food crops around Pb–Zn mining localities in Enyigba, southeastern Nigeria. *Journal of African Earth Sciences* 116: 182-189. DOI: 10.1016/j.jafrearsci.2015.12.025.
- Odukoya, A.M., Olobaniyi, S.B., Abdussalam, M. (2016). Metal pollution and health risk assessment of soil within an urban industrial estate, southwest Nigeria. *Ifè Journal of Science* 18(2): 573 – 583.
- Pająk, M., Halecki, W., Gasiorek, M. (2015). Accumulative response of Scots pine (*Pinus sylvestris* L.) and silver birch (*Betula pendula* Roth) to heavy metals enhanced by Pb–Zn ore mining and processing plants: Explicitly spatial considerations of ordinary kriging based on a GIS approach. *Chemosphere* 168: 851–859. DOI: 10.1016/j.chemosphere.2016.10.125.
- Pontius, G.R., and Malanson, J. (2005) Comparison of the structure and accuracy of two land change models. *International Journal of Geographical Information Science* 19(2): 243-265. DOI: 10.1080/13658810410001713434.
- Pontius, Jr. R. G., and Millones, M., (2011). Death to Kappa: birth of quantity disagreement and allocation disagreement for accuracy assessment. *International Journal of Remote Sensing* 32 (15): 4407–4429. <https://doi.org/10.1080/01431161.2011.552923>.
- Ralha, C.G., Abreu, C.G., Coelho, C.G.C., Zaghetto, A., Macchiavello, B., Machado, R.B. (2013). A multi-agent model system for land-use change simulation. *Remote Sensing of Environment* 42: 30–46. <https://doi.org/10.1016/j.envsoft.2012.12.003>.

- Shahidul Islam, M.D., and Ahmed, R. (2011). Land-use change prediction in Dhaka city using GIS aided Markov chain modeling. *Journal of Life and Earth Science* 6: 81-89.
- Shamsi, S.R.F., (2010). Integrating Linear Programming and Analytical Hierarchical Processing in Raster-GIS to Optimize Land Use Pattern at Watershed Level. *Journal of Applied Sciences and Environmental Management* 14(2): 81-5.
- Singh, S.K., Mustak, S., Srivastava, P.K., Szabo, S., Islam, T. (2015). Predicting Spatial and Decadal LULC Changes Through Cellular Automata Markov Chain Models Using Earth Observation Datasets and Geo-information. *Environmental Processes* 2(1):61-78.
- Sohl, T.L., and Claggett, P.R. (2013). Clarity versus complexity: Land-use modeling as a practical tool for decision-makers. *Journal-Environ Manage* 129: 235-43. PMID:23954777. <https://doi.org/10.1016/j.jenvman.2013.07.027>.
- Soil survey staff. (2010). Keys to soil taxonomy,. Washington D. C.: USDA soil conservation service revised edition (9th).
- Stefanov W.L., Ramsey M.S., Christensen P.R. (2001). Monitoring urban land cover change: An expert system approach to land cover classification of semiarid to arid urban centers. *Remote Sensing of Environment* 77 (2): 173-85.
- Su, C., Jiang, L., Zhang, W. (2012). A review on heavy metal contamination in the soil worldwide: Situation, impact and remediation techniques. *Environmental Skeptics and Critics* 3(2): 24-38. <https://doi.org/10.1016/j.envint.2014.04.014>.
- Sun, Y., Zhou, Q., Xie, X., Liu, R. (2013). Spatial, sources and risk assessment of heavy metal contamination of urban soils intypical regions of Shenyang, China. *Journal of Hazardous Materials* 174(1-3): 455-462. DOI: 10.1016/j.jhazmat.2009.09.074.
- Sutherland, R. (2000). Bed sediment-associated trace metals in an urban stream, Oahu, Hawaii. *Environmental Geology* 39(6): 611-627. DOI: 10.1007/s002540050473.
- Story, M., and Congalton, R.G. (1986) Accuracy Assessment: A User's Perspective. *Photogrammetric Engineering and Remote Sensing* 52: 397-399.
- Tiani, A.M., Besa, M.C., Devisscher, T., Pavageau, C., Butterfield, R., Bharwani, S. Bele, M. (2015). Assessing Current Social Vulnerability to Climate Change: A Participatory Methodology. Working Paper 169. Bogor: Center for International Forestry Research.
- Tijani, M.N., Kenneth, J., Yoshinar, H. (2004). Environmental impact of heavy metals distribution in water and sediment of Ogunpa River, Ibadan area, South Western Nigeria. *Journal of Mining and Geology* 40(1): 73 - 83. DOI: 10.4314/jmg.v40i1.18811.
- Tobore, A., Senjobi B., Ogundiyi, T., Samuel, B. (2021). Geospatial assessment of wetlands soils for rice production in Ajibode using Geospatial Techniques. *Open Geosciences* 13: 310-320. <https://doi.org/10.1515/geo-2020-0227>.
- Udo, E.J., Ibia, T.O., Ogunwale, J.A., Ano, A.O., Esu, I.E. (2009). *Manual of soil, plant and water analyses*. Lagos: Sibon Books Ltd 183 pp.
- United Nations. (2008). *World Urbanization Prospects: The Revision United Nations (Population Division of the Department of Economic and Social Affairs) New York.ESA/P/WP/224,2012*.
- Uriah, L.A., and Shehu, U. (2014). Environmental risk assessment of heavy metals content of municipal solid waste used as organic fertilizer in vegetable gardens on the Jos Plateau, Nigeria. *American Journal of Environmental Protection* 3(6 - 2): 1 - 13.
- Walkley, A., and Black, I. A. (1939). An examination of the Degtjareff method for determining soil organic matter and a proposed modification of the chromic acid titration method. *Soil Science* 37:29 -38. DOI: 10.1097/00010694193401000-00003.
- Wali, E., Phil-Eze, P.O., Nwankwoala, H.O., Bosco-Abiahu, L.C., Emelu, V.O., (2019). Analysis of land use and land cover changes in the wetland ecosystem of Port-Harcourt metropolis, Nigeria. *International Journal of Ground Sediment and Water* 9: 503-524.
- Waswa, B. S., Vlek, P. L., Tamene, L. Okoth, P. F. (2012). Mapping land degradation patterns using NDVI as a Proxy: a case study of Kenya. *Resilience of Agricultural Systems Against Crises (Tropentag, September 19-21 2012), Göttingen-Kassel/Witzenhausen*.
- Wu, C.D., Cheng, C.C., Lo, H.C., Chen, Y.K. (2010). Application of SEBAL and Markov Models for Future Stream Flow Simulation Through Remote Sensing. *Water Resource Manag.* 24(14): 3773-97. <https://doi.org/10.1007/s11269-010-9633-9>.
- Weng, Q., and Yang, S. (2004). Managing the adverse thermal effects of urban development in a densely populated Chinese city. *Journal of Environmental Management* 70: 145-156.
- Xiao, J., Shen, Y., Ge, J., Tateishi, R., Tang, C., Liang, Y. (2006). Evaluating urban expansion and land-use change in Shijiazhuang, China by using GIS and remote sensing. *Landscape and Urban Planning* 75: 69-80. <http://dx.doi.org/10.1016/j.landurbplan.2004.12.005>.
- Yang, X., Zheng, X., Lv, L. (2012). A spatiotemporal model of land use change based on ant colony optimization, Markov chain and cellular automata. *Ecol Model* 233:11-19. doi:10.1016/j.ecolmo del.2012.03.011.
- Zhang, J., Niu, J., Bao, T., Buyantuyev, A., Zhang, Q., Dong, J., Zhang, X. (2015). Human-induced dry-land degradation in Ordos plateau, China, revealed by multi-level statistical modelling of normalized difference vegetation index and rainfall time series. *Journal of Arid Land* 6: 219-229. <https://doi.org/10.1007/s40333-0130203-x>.